Thermal Investigation in the Cappadocia Region, Central Anatolia-Turkey, Analyzing Curie Point Depth, Geothermal Gradient, and Heat-Flow Maps from the Aeromagnetic Data

Funda Bilim,[1] Sinan Kosaroglu,[1] Attila Aydemir,[2] and Aydin Buyuksarac[3]

Abstract—In this study, curie point depth (CPD), heat flow, geothermal gradient, and radiogenic heat production maps of the Cappadocian region in central Anatolia are presented to reveal the thermal structure from the aeromagnetic data. The large, circular pattern in these maps matches with previously determined shallow (2 km in average) depression. Estimated CPDs in this depression filled with loose volcano-clastics and ignimbrite sheets of continental Neogene units vary from 7 to 12 km, while the geothermal gradient increases from 50 to 68 °C/km. Heat flows were calculated using two different conductivity coefficients of 2.3 and 2.7 $Wm^{-1} K^{-1}$. The radiogenic heat production was also obtained between 0.45 and 0.70 $\mu W\ m^{-3}$ in this area. Heat-flow maps were compared with the previous, regional heat-flow map of Turkey and significant differences were observed. In contrast to linear heat-flow increment through the northeast in the previous map in the literature, produced maps in this study include a large, caldera-like circular depression between Nevsehir, Aksaray, Nigde, and Yesilhisar cities indicating high geothermal gradient and higher heat-flow values. In addition, active deformation is evident with young magmatism in the Neogene and Quaternary times and a large volcanic cover on the surface. Boundaries of volcanic eruption centers and buried large intrusions are surrounded with the maxspots of the horizontal gradients of magnetic anomalies. Analytic signal (AS) map pointing-out exact locations of causative bodies is also presented in this study. Circular region in the combined map of AS and maxspots apparently indicates a possible caldera.

Key words: Curie point depth, geothermal gradient, heat flow, Cappadocia, caldera.

1. Introduction

The world-wide known touristic Cappadocia region with its fairy-chimneys is located in the central Anatolia between Aksaray, Nigde, and Nevsehir towns in Turkey. The surface of Cappadocia is covered by the Cappadocian Volcanic Complex (CVC) under the influence of the Alpine Orogeny and active tectonics represented by the Sereflikochisar–Aksaray Fault (SAF) to the west and Ecemis Fault (EF) to the east (Figs. 1, 2). CVC was formed after two major (Neogene and Quaternary) magmatic episodes above the metamorphic basement of the Kirsehir Block. Many central Anatolian basins are surrounding CVC; the Tuzgolu (Salt Lake) Basin to the W and SW, Haymana Basin to the northwest, Kirikkale Basin to the north, Sivas Basin to the northeast (Aydemir and Ates 2005, 2006; Aydemir 2008, 2009; Onal et al. 2008). A simplified geological map of the region is presented in Fig. 2.

The study area, particularly CVC has been investigated with the geological and geophysical purposes since 1964 (Sassano 1964). Because the surface is covered by young volcanic rocks, these investigations were generally focused on the volcanoes, volcano-sedimentary units, cinder cones, calderas, and structural–evolutionary characteristics of the volcanic units (Pasquare 1968; Innocenti et al. 1975; Batum 1978a, b; Ekingen, 1982; Bas et al. 1986; Pasquare et al. 1988; Le Pennec et al. 1994; Toprak 1998; Piper et al. 2002, 2013; Aydemir, 2009). These investigations are sometimes based on the different geophysical data and methods such as gravity, aeromagnetic, electrical sounding, and electromagnetic and geothermic

[1] Department of Geophysical Engineering, Cumhuriyet University, 58140 Sivas, Turkey.
[2] Turkish Petroleum Corp, Sogutozu Mah. 2180. Cad. No: 10, Sogutozu, Ankara, Turkey. E-mail: aydemir@tp.gov.tr; attila.aydemir@gmail.com
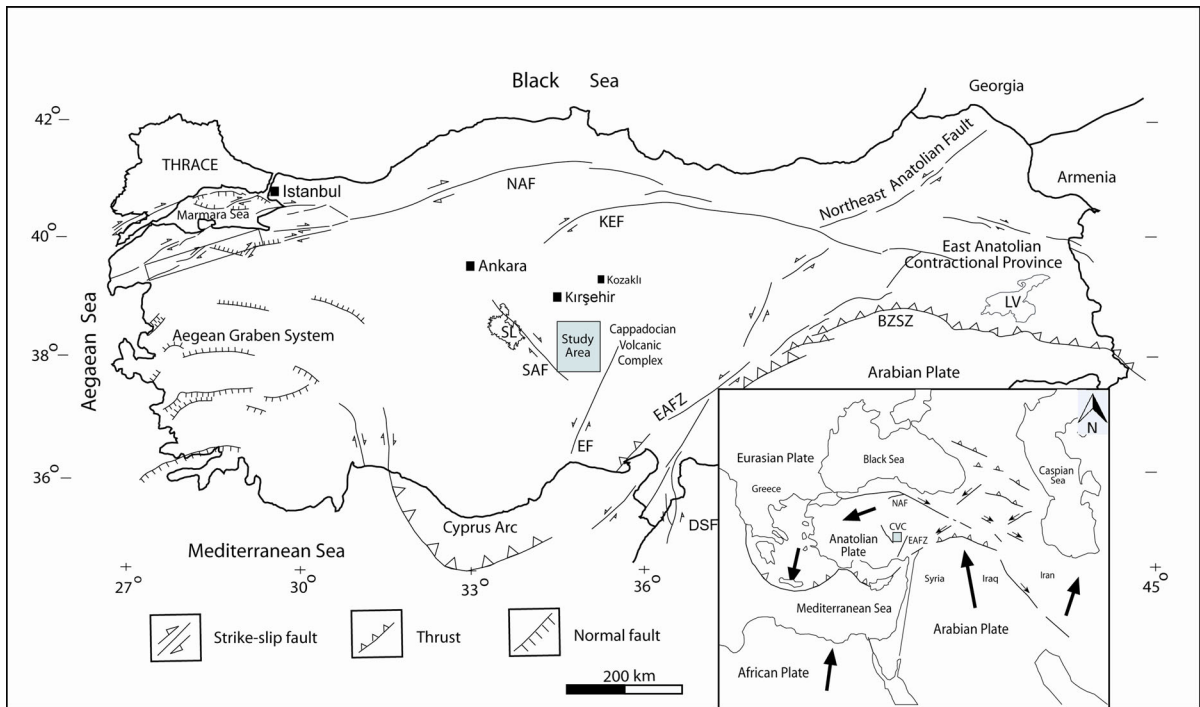[3] Department of Civil Engineering, Bitlis Eren University, 13000 Bitlis, Turkey.

Figure 1

Location map of the study area in the tectonic framework of Turkey and its surroundings region (modified from Platzman et al. 1998). *NAF* North Anatolian Fault, *SL* Salt Lake, *LV* Lake Van, *EAFZ* East Anatolian Fault Zone, *DSF* Dead Sea Fault, *BZSZ* Bitlis–Zagros Suture Zone, *SAF* Sereflilochisar–Aksaray Fault, *EF* Ecemis Fault, *KEF* Kirikkale–Erbaa Fault, *CVC* Cappadocian Volcanic Complex. After Kosaroglu et al. (2016)

methods (i.e., Ilkisik et al. 1997; Froger et al. 1998; Ates et al. 2005; Buyuksarac et al. 2005; Kosaroglu et al. 2016). According to the results of these studies, it is possible to claim that the region has a modest geothermal potential and some places with possible undiscovered geothermal fields. The initial Curie point depth (CPD) investigation was performed in central Anatolia entirely by Ates et al. (2005). In addition, deep structure of CVC was revealed by Buyuksarac et al. (2005) using the aeromagnetic and gravity anomalies where a large, deep-seated magnetic anomaly was determined under this region. Top of the causative body was found at 4 km and bottom at 5.7 km as the source of volcanic rocks on the surface. Recently, Kosaroglu et al. (2016) investigated the shallow structures and causative bodies for the gravity and magnetic anomalies in the region. They found two separate shallow structures having 2 km bottom depth and about 0.3 km top depth from the spectral

analysis. In addition, they determined almost circular depression beneath CVC with dimension of 70×50 km^2 that could be a large caldera to produce high heat flow for the geothermal potential of this region.

This paper includes the successive investigation of the above-mentioned caldera-like structure with geothermal purposes and it may be considered as the continuation paper of Kosaroglu et al. (2016). In this study, CPD, geothermal gradient, heat flow, radiogenic heat production, and Analytic Signal together with the maxspots maps were prepared using the aeromagnetic data of the Cappadocian region. The method to identify CPD from the magnetic anomalies is based on the theories of Spector and Grant (1970) and Okubo et al. (1985), and it is a well-known technique for obtaining the thermal structure of the crust. The method is explained with the assumption that the summation of responses from the independent, rectangular vertical prisms creates the magnetic anomaly. In the stages of

the method, top depth and depth to the centroid of a magnetic source are calculated, and then, CPDs where the thermal state exceeds the Curie temperature (580 °C) are estimated. Then, geothermal gradient, heat flow, and radiogenic heat production maps can be constructed from the CPD values successively. In this research, all these values and produced maps were correlated with each other and a well consistency was observed between them.

2. Geology of Cappadocia Region

A summarized, brief description about the geological units in the Cappadocian region will be given in this study, because details can be found from the previous paper of authors (Kosaroglu et al. 2016). Metamorphics of the Kirsehir Block constitute the basement in the study area together with the ultramafics and acidic intrusions (Seymen 1982). The
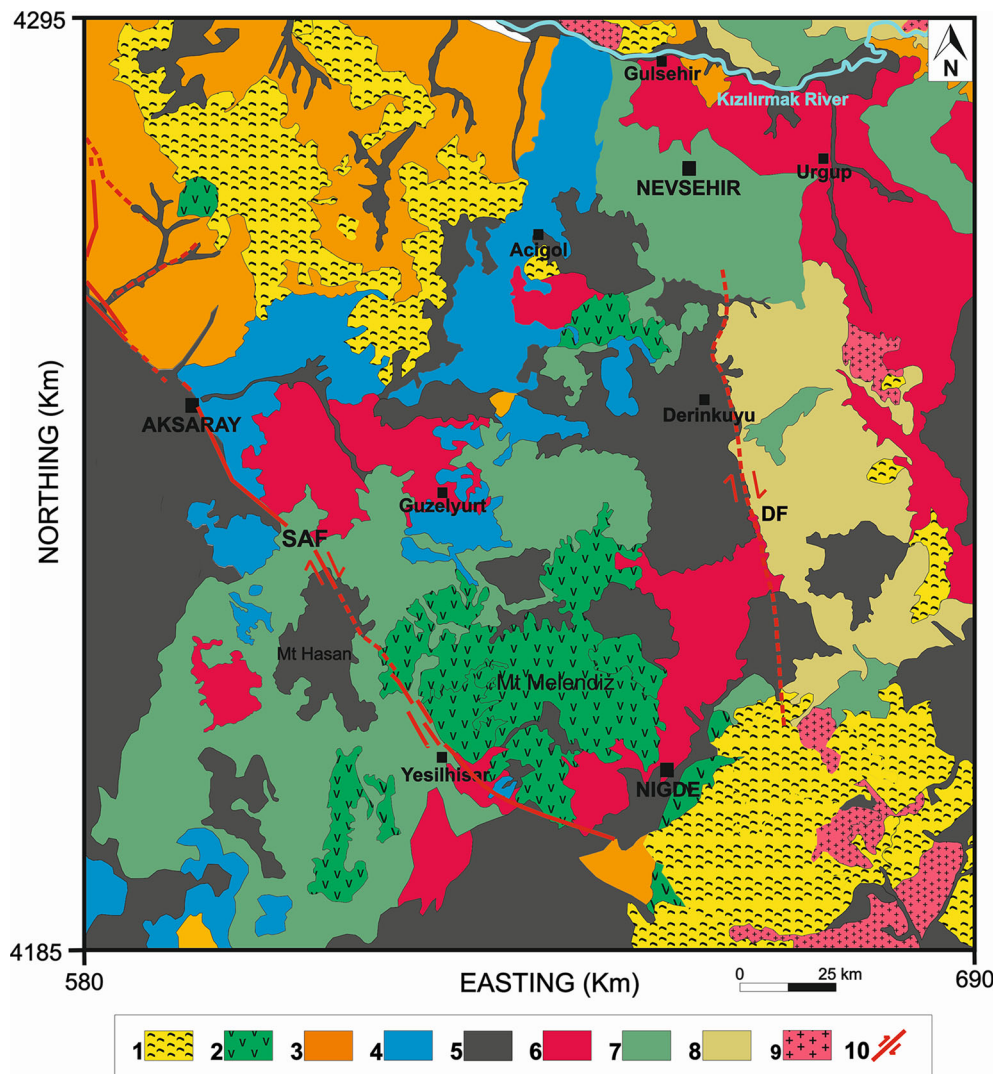

Figure 2
Simplified geological map of Cappadocia (modified from Temel et al. 1998). *SAF* Sereflikochisar–Aksaray Fault, *DF* Deliler Fault. 1: Basement rocks, 2: Mio-Pliocene volcanic complex, 3: Ignimbrite and coeval terrestrial sediments, 4: Main Quaternary Monogenic volcanism, 5: Young Quaternary sedimentary and volcanic units, 6: Undifferentiated U. Miocene-Pliocene pyroclastics, 7: U. Miocene pyroclastics, 8: Pliocene pyroclastics, 9: U. Cretaceous granodiorites, 10: Faults. After Kosaroglu et al. (2016). Coordinate system is UTM (Zone: 36)
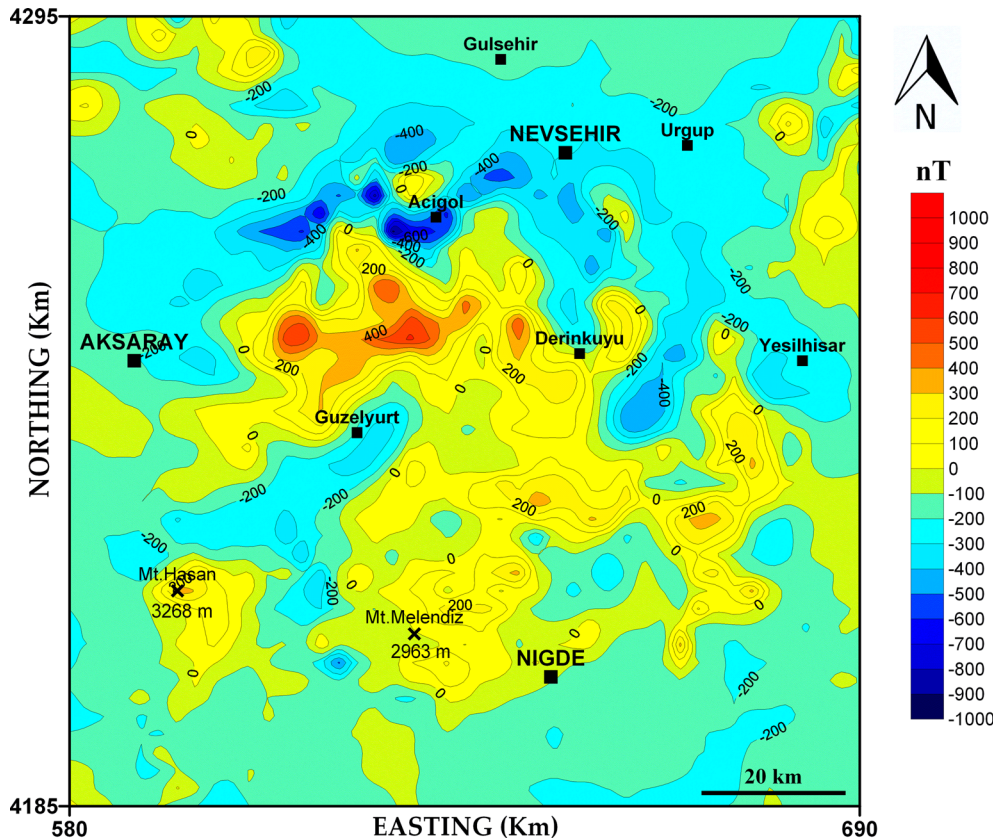
Figure 3
Magnetic anomaly map of the Cappadocian region. Contour interval: 100 nT. After Kosaroglu et al. (2016). Coordinate system is UTM (Zone: 36)

Karakaya ultramafics in the form of ophiolite nappes overlie the Kirsehir metamorphics (Bingol 1974). However, the Baranadag Pluton is the most significant magmatic intrusion in the central Anatolia.

Volcanic rocks in CVC from Aksaray to Kayseri are composed of Neogene ignimbrites, and lava-ash flows and tuffs of Mount Melendiz and Mount Hasan (Innocenti et al. 1975; Besang et al. 1977; Bigazzi et al. 1993). The Karakaya Formation was deposited in fluvial and lacustrine environments accompanied by a regional uplift in the silent period between the eruptions (Ayhan and Papak 1988). The volcanic activity commenced again after the sedimentation of Karakaya Formation and Selime tuffs; Gelveri and Kizilkaya ignimbrites were emplaced (Innocenti et al. 1975; Besang et al. 1977), but the volcanic activity ceased again until the Quaternary. The last re-activation of volcanism started by the emplacement of Acigol rhyolites and obsidians, and by the lava eruptions of Mt.

Hasan and Mt. Melendiz that terminated with the olivine basalt flows (Bigazzi et al. 1993).

There are very significant volcanoes in the region such as the Mt. Melendiz Volcano (Fig. 2). The volcanics erupted from this volcano are grouped as "Melendiz Volcanites" (Besang et al. 1977). The other important volcano is the Mt. Hasan Volcano (Fig. 2) having three different eruption centers in a short radius. Volcanic eruptions from this mountain are composed of tuffs, ashes, and cinder pebbles covered by andesitic and dacitic lava flows. The youngest volcanics are mainly originated from the basalt eruptions lying on relatively flat areas (Aydar and Gourgaud 1998).

3. Aeromagnetic Data of Cappadocia Region

The potential field (aeromagnetic) data in the study area were obtained from the General Directory
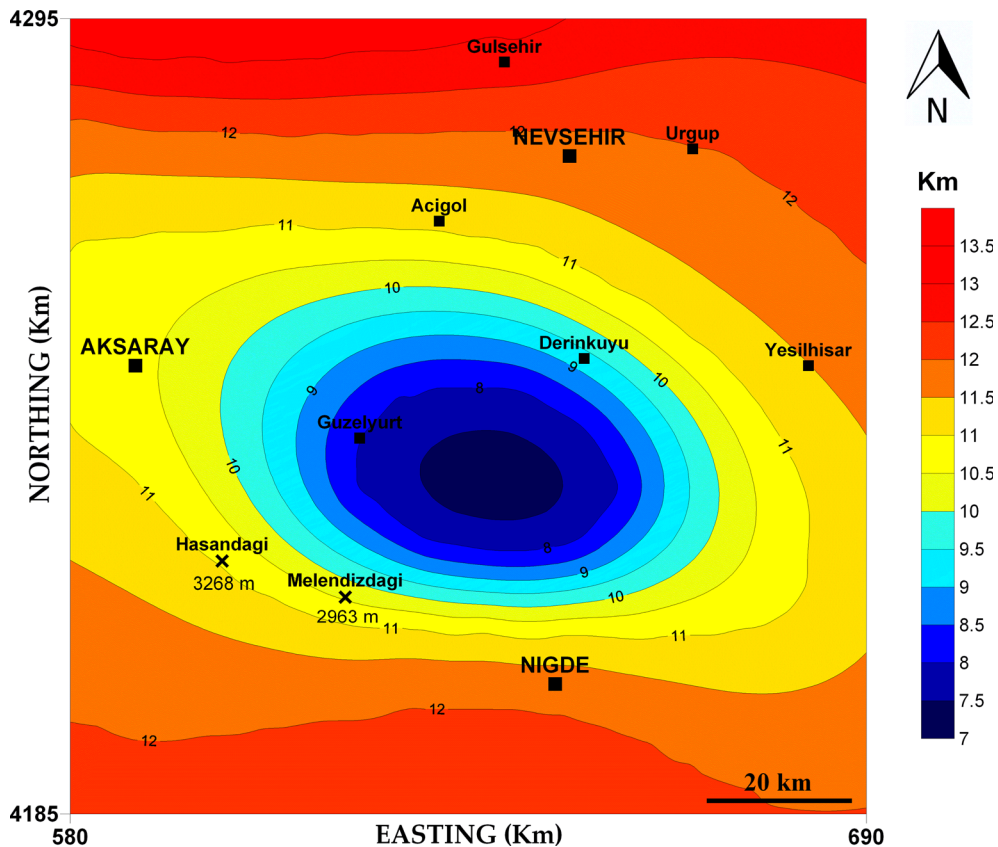
Figure 4
Curie Point Depth (CPD) map of the Cappadocian region. Contour interval: 0.5 km. Coordinate system is UTM (Zone: 36)

of Mineral Exploration and Research of Turkey (MTA) after all corrections applied onto the measurements and data were reduced to the reference values.

Aeromagnetic data were collected by a contractor aero-service company on behalf of MTA. Total component of the geomagnetic field was measured along the 2 km distant profiles in the N–S directions. The flight altitude is approximately 600 m (2000 ft). Distance between flight lines is generally 1–2 km and sampling interval is about 70 m. Survey measurements were adapted to October 1982 values after daily variation-direction error corrections. The residual magnetic anomaly map after removal of "International Geomagnetic Reference Field-IGRF" values is given in Fig. 3. The program of Baldwin and Langel (1993) was used for the removal process. Inclination and declination angles in the study area

are taken as 55° and 4°, respectively. The aeromagnetic anomalies range from about −600 nT around Acigol to 500 nT in the area between Acigol and Guzelyurt (Fig. 3). Detailed information about the potential field data can be found in Kosaroglu et al. (2016).

4. Construction of CPD, Geothermal Gradient, Heat Flow, and Crustal Radiogenic Heat Production Maps

CPD describes the specific depth where the magnetic minerals in the crust lost their magnetic property above a certain temperature and they are transformed from the ferromagnetic state to paramagnetic state. In the isotherm studies, the Curie temperature of pure magnetite is accepted 580 °C
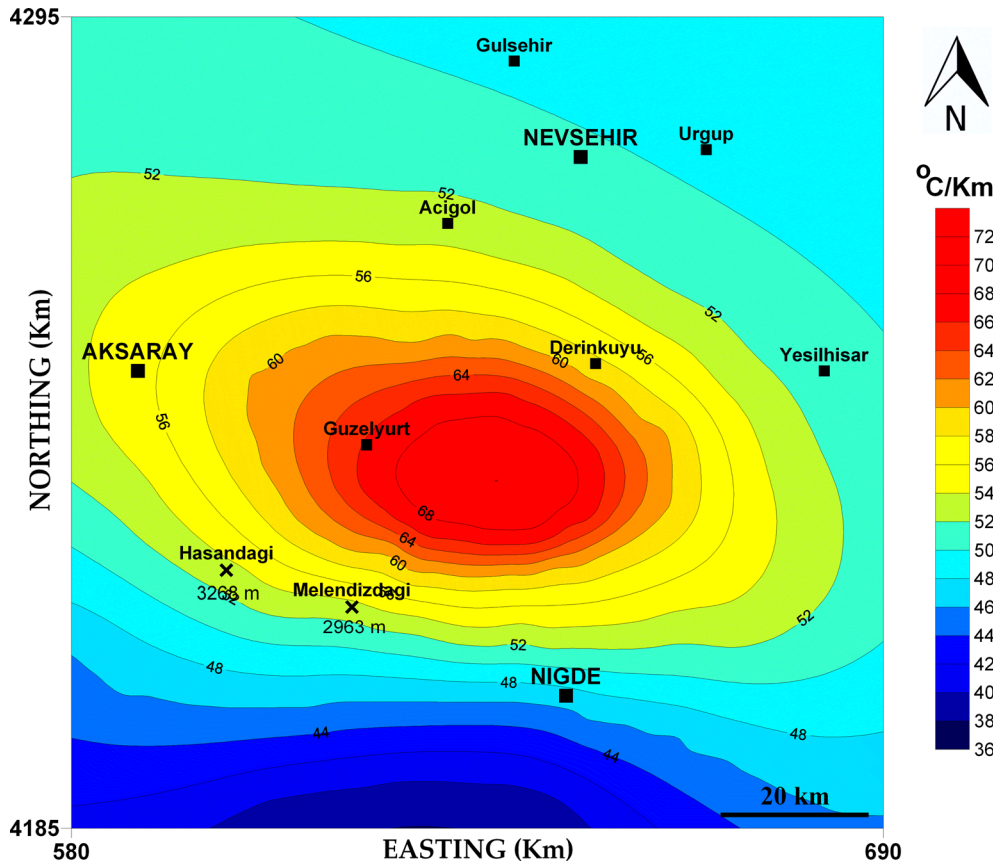
Figure 5
Geothermal gradient maps of the Cappadocian region calculated from the Curie point depths. Contour interval is 2 °C km^{-1}. Coordinate system is UTM (Zone: 36)

(e.g., Okubo et al. 1985; Schlinger 1985; Hunt et al. 1995; Tanaka et al. 1999; Stampolidis and Tsokas 2002; Rozimant et al. 2009). In accordance with this assumption, Schlinger (1985), Frost and Shive (1986), and Ross et al. (2006) pointed out that 580 °C may be considered as a reasonable crustal Curie temperature value for the continental areas.

The method to estimate CPDs from the aeromagnetic anomaly data by Okubo et al. (1985) was used in this study. This method is based on the calculation of the depth of a magnetic source from the power spectrum of magnetic anomalies after transformation of data into frequency domain. The top and centroid depths of the magnetic sources are given as z_t and z_0 by Okubo et al. (1985), respectively. Then, Curie depths (z_b) are estimated using the equation of $z_b = 2z_0 - z_t$ (Okubo et al. 1985, 1989).

There are some published CPD investigations in different regions in Turkey, particularly in the geothermally prospective Aegean region (i.e., Dolmaz et al. 2005a, b; Bilim et al. 2016). CPD map of the central Anatolia was initially prepared by Ates et al. (2005) according to the aeromagnetic anomalies. However, it was a regional map and does not indicate local details such as in the Cappadocia Region. Although CPD map given in this study is the succession of Ates et al. (2005) and consistent with the regional map, in general, it was re-constructed by calculating particularly from the Cappadocia Region's magnetic anomalies. Because of this reason, it indicates more details accurately. CPD map of the Cappadocia Region is presented in Fig. 4. On the contrary, the CPD anomaly is composed of a unique, large anomaly located in the center of study area,
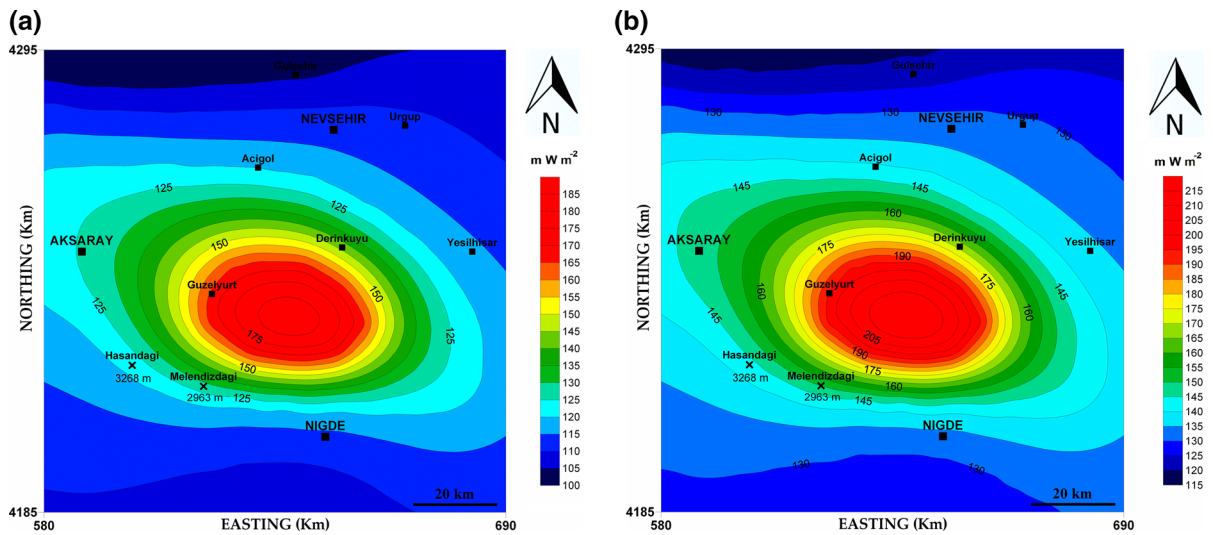
Figure 6

Heat-flow maps of the Cappadocian region. **a** For thermal conductivity 2.3 W m^{-1} K^{-1}; **b** for thermal conductivity 2.7 W m^{-1} K^{-1}. Contour interval is 5 mW m^{-2}. Coordinate system is UTM (Zone: 36)

although the magnetic anomaly has many complexities distributed randomly. From this point of view, it may be suggested that all these anomalies were arised from only one, large source at depth.

Geothermal gradient can be calculated from CPD values using the following formula (Okubo et al. 1985, 2005; Tsokas et al. 1998; Ates et al. 2005; Hsieh et al. 2014):

$$\text{grad } T = 580°C/\text{Curie depth.}$$

The geothermal gradient map of the study area was produced using this formula and given in Fig. 5.

In a successive process, the surface heat flow is calculated from the geothermal gradient. In the estimation of the thermal structure of the lithosphere, the steady-state solution of the thermal conductivity equation, $\nabla^2 T = -A/k$, is used.

$A = A(z)$ is the heat production as a function of depth (z), and similarly, $k = k(z)$ is the thermal conductivity as a function of depth (z).

The boundary conditions for this calculation are given by Turcotte and Schubert (1982) and Artemieva and Money (2001) as follows:

$$T|_{z=0} = 0$$
$$q_0 = -k\frac{\partial T}{\partial z}. \tag{1}$$

Here, q_0 is the surface heat flow and $\frac{\partial T}{\partial z}$ is the thermal gradient.

The thermal conductivity coefficient varies between 2.5 and 3.0 Wm^{-1} K^{-1} for upper parts of the crust and between 2.6 and 2.8 Wm^{-1} K^{-1} for the middle parts (Springer, 1999). The heat-flow values in this investigation were estimated using two different coefficients of 2.3 and 2.7 Wm^{-1} K^{-1} (Fig. 6a, b). 2.3 Wm^{-1} K^{-1} was chosen to see the lower limit of upper crust (less than the given coefficient by Springer 1999) and 2.7 Wm^{-1} K^{-1} was preferred as the average coefficient for the upper and middle crust, both. As expected, high heat-flow regions have an inverse relationship with shallower CPDs, in contrast to lower heat-flow regions associated with deeper CPDs.

The radiogenic heat production is the heat-flow contribution of the radioactive minerals in the continental crust after the decay processes. Heat production of these minerals is depth-dependent. Crustal radiogenic heat production in the Earth is mostly resulted from the decay of Uranium-235 (^{235}U), Uranium-238 (^{238}U), Thorium-232 (^{232}Th), and Potassium-40 (^{40}K). Radiogenic heat production (A) formula can be given as follows:
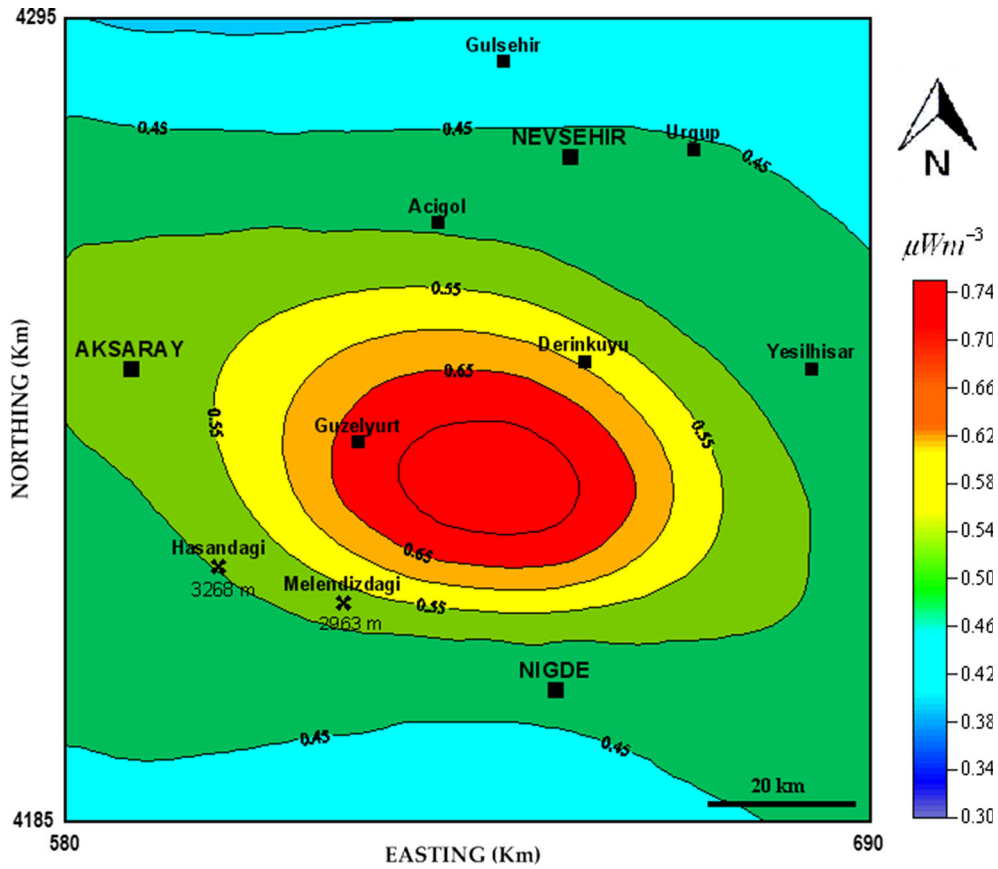
$$A(z) = A_0 \exp(-z/D). \tag{2}$$

Figure 7
Variation of the crustal radiogenic heat production in the Cappadocian region. Contour interval is 0.5 μW m^{-3}. Coordinate system is UTM (Zone: 36)

Here, A_0 is the radiogenic heat production rate on the surface of the Earth, z is depth, and D is the radiogenic scaling depth (Lachenbruch 1970).

The radiogenic heat production (A) map for the estimated CPDs is presented in Fig. 7 where the coefficient D is assumed as 10 km (Lachenbruch 1970; Jaupart 1986), while coefficient A_0 is taken 1.5 μW m^{-3} (Springer 1999).

5. Analytic Signal (AS) Transformation and Maxspots of the horizontal Gradients of the Magnetic Anomalies

Approximate locations of the causative bodies are determined with the transformation of aeromagnetic anomalies to the Analytic Signal (AS). The AS can be calculated three dimensionally with the sum of the vertical and horizontal gradients given by the following:

$$A(x,y) = \frac{\partial M}{\partial x}i + \frac{\partial M}{\partial y}j + \frac{\partial M}{\partial z}k, \qquad (3)$$

where M is the magnitude of magnetic anomaly; i, j, and k are unit vectors in the x, y, and z directions (Nabighian 1972; MacLeod et al. 1993; Salem et al. 2002; Bilim and Ates 2003, 2005; Saibi et al. 2006; Ortiz-Aleman and Urrutia-Fucugauchi 2010).

The AS amplitude is formulated as follows;

$$|A(x,y)| = \sqrt{\left(\frac{\partial M}{\partial x}\right)^2 + \left(\frac{\partial M}{\partial y}\right)^2 + \left(\frac{\partial M}{\partial z}\right)^2}. \qquad (4)$$

AS map of the study area is given in Fig. 8 and locations of the causative bodies are represented with dark patches. As observed in the magnetic anomaly
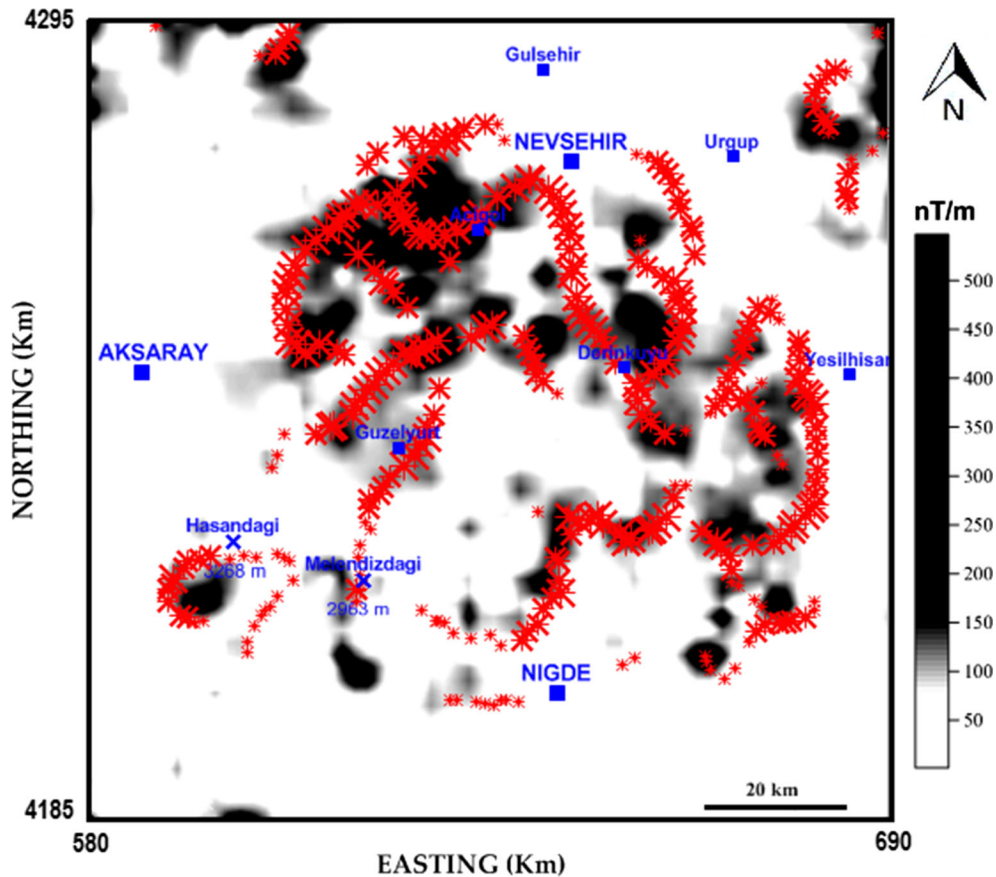
Figure 8
Black–white (gray image) map shows the analytic signal (AS) map applied to the Cappadocian region. Asteriks in the red colour indicate the locations of maxima of horizontal gradients. Coordinate system is UTM (Zone: 36)

map (Fig. 3), magnetic anomalies are distributed all over the Cappadocia region. However, there is an empty sector surrounded with lowest CPD contours (7.5–8 km) between Derinkuyu and Guzelyurt (Fig. 4).

In addition to AS transformation, maxspots representing the horizontal gradients of magnetic anomalies were applied onto the AS map to display alignments along the causative bodies and their boundaries (Fig. 8). In general, these maxspots are emplaced along the old magmatic intrusions that are probably cold. However, they surround the above-mentioned empty region with no AS anomalies. As they indicate nearly largest horizontal gradient (maxima) along the vertical boundaries or along the edge of causative bodies, this irregular circular boundary could reflect the crater of a large caldera.

For the mathematics of horizontal gradient maxima, Blakely's (1996) book can be given as a key reference.

6. Conclusions and Discussion

The Cappadocian region is a well-known touristic destination in Turkey with its fairy-chimneys, tuff-cones, early Christian churches carved in these tuff-cones, underground cities, spectacular narrow valleys created by fluvial, eolian, and anthropogenic processes. All these natural and associated anthropogenic beauties are originated from the volcanic rocks on the surface/subsurface geology of Cappadocia. Each year, thousands of tourists from all over the world visit these cities and many people are
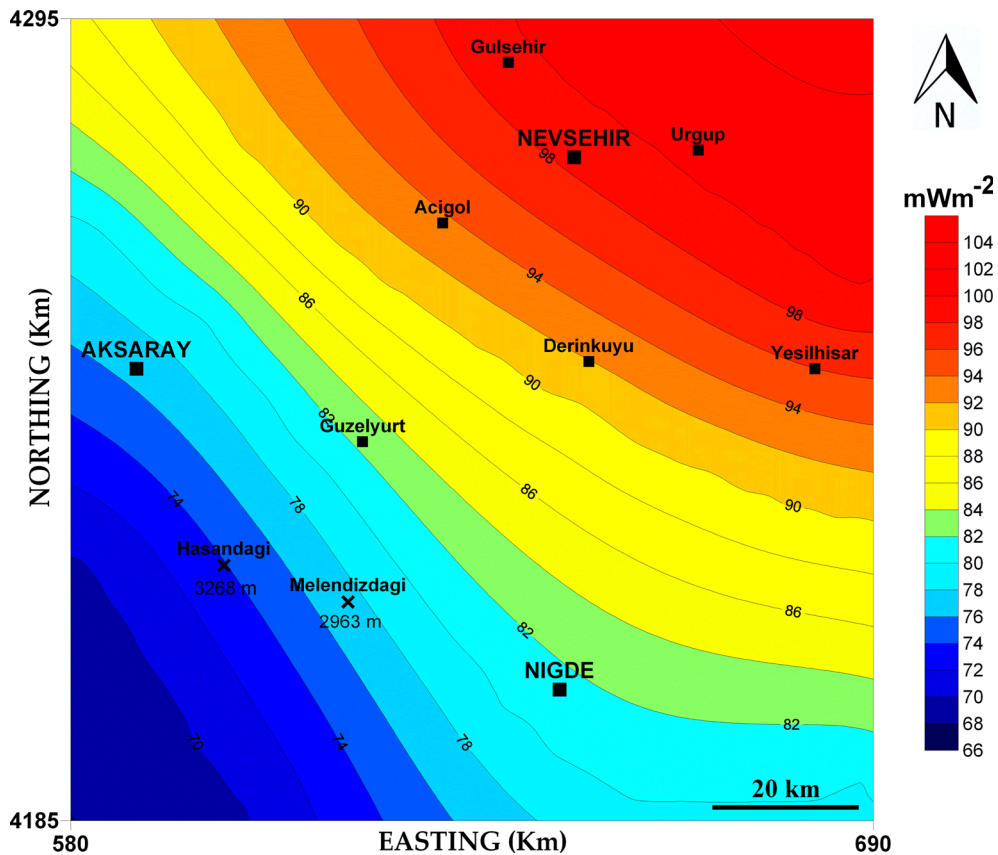
Figure 9
Surface heat-flow map of the Cappadocian region (modified from Tezcan and Turgay, 1987). Contour interval is 2 mW m^{-2}. Coordinate system is UTM (Zone: 36)

aware of the abundance of different prosperities of Cappadocian region. However, there may be another possible underground (subsurface) wealth in the region; it is the geothermal potential. There are some hot springs allowing the health resort investments, particularly in and around Kirsehir, Kozakli, and other cities to the north of the study area. In this study, an evaluation for the geothermal potential of Cappadocia was approximated using the magnetic anomalies in the region. This manuscript is a follow-up paper that was published very recently to investigate the shallow structures and possibility of a large caldera or existence of multiple calderas throughout the region (Kosaroglu et al. 2016).

Mt. Melendiz and Mt. Hasan are two volcanic mountains located to the W and SW of large depression that was filled with ignimbrites, tuffs and ashes discharged from the eruption of these

mountains. The average depth of this large depression was found about 2 km from the spectral analysis and 2D–3D modeling study. We do not have enough evidences to accept this depression as a super-caldera in contrast to existence of already defined small calderas in the study area. However, CPDs in this sector are very low, changing between 7 and 12 km. The shallower CPD sector is located between Derinkuyu, Guzelyurt, Mt. Melendiz, and Nigde represented with contours of 7–8 km (Fig. 4). This part does not coincide with the deepest part of the depression that was estimated around 2.7 km in the 3D map (Kosaroglu et al. 2016). In contrast, it partly overlaps a subsurface high that is surrounded by a super-caldera shape depression. The most striking characteristic of shallow CPD region is that it is not apparently represented by a gravity or magnetic anomaly (Kosaroglu et al. 2016). In accordance with

the CPD map, geothermal gradient values increase up to 68 °C/km (Fig. 5). Heat-flow maps indicate highest values of 180 (Fig. 6a) and 210 mW m^{-2}(Fig. 6b) for the thermal conductivity coefficients of 2.3 and 2.7 Wm^{-1} K^{-1}, respectively. All these maps are consistent with each other, because they are the derived from the magnetic anomaly data. Heat-flow estimations in this research may be correlated with the previous, regional heat-flow map prepared for Turkey, entirely (Tezcan and Turgay 1987). Because the map of Tezcan and Turgay (1987) is a regional map, it does not include the details for any specific region. In the study area, their map indicates a linear increase of heat flow from the southwestern corner to the NE in the range of 70–102 mW m^{-2}, and there is not an oval heat-flow anomaly region between Derinkuyu, Guzelyurt, Mt. Melendiz, and Nigde in their map, either (Fig. 9). In addition, heat-flow values are very low (up to 102 mW m^{-2}) in comparison with the highest values obtained in this research (180
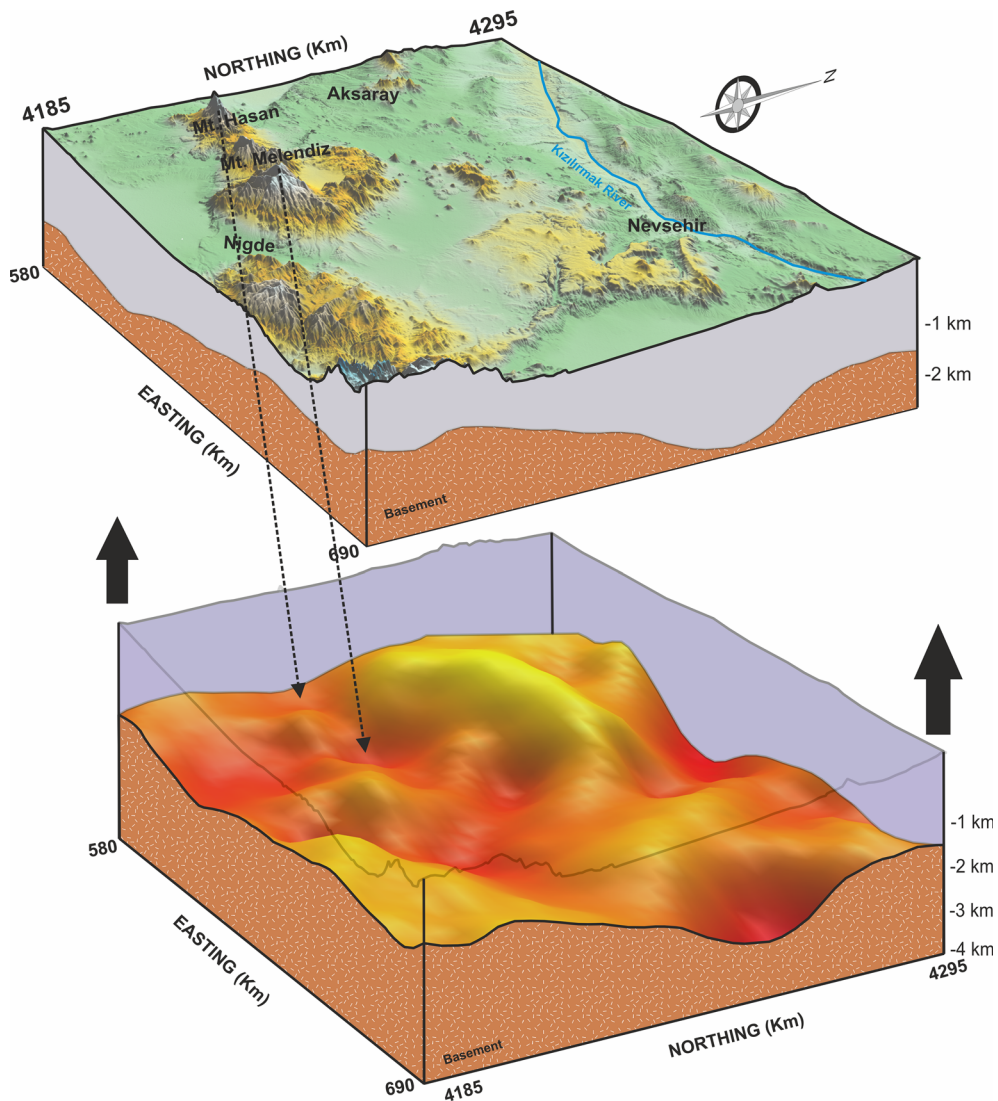

Figure 10
Block diagram of the subsurface shallow structure and basement beneath the surface topography including two significant volcanic mountains in the Cappadocian region. Above: Topography and cover units' thickness (indicated with gray colour) down to the shallow structure of Cappadocia; below: shallow structure and the basement

mW m^{-2} for the thermal conductivity coefficient of 2.3 Wm^{-1} K^{-1} and 210 mW m^{-2} for 2.7 Wm^{-1} K^{-1}). In addition to the heat flow from the deeper parts of the crust, radiogenic heat production from the radioactive minerals was also calculated from the magnetic anomaly data (Fig. 7). This map also indicates an anomalous high heat production in the same part of the study area. Naturally, this is an expected consequence, because it is another useful approximation using the same set of data. Radiogenic heat production varies from 0.45 to 0.70 μW m^{-3}.

Horizontal gradients of the magnetic anomalies display boundaries of causative bodies. Similarly, Analytic Signal (AS) displays the approximate locations of the causative bodies, because it is the sum of the vertical and horizontal gradients in three dimensions. If the AS anomaly and maximas of horizontal gradients match at the same location, they may indicate a causative body or steeply dipping locations of old intrusions. However, if they both surround a magnetic anomaly free zone with small acreage, it may indicate a magma chamber of an active caldera surrounded by old eruptions or it may be a magma chimney of a large volcanic zone that was recently transferred to an inactive phase but not cold enough to create a magnetic anomaly. The oval zone in the NE–SW direction observed in the study area can be classified with the above-mentioned definitions in the combo map of AS and maxspots (Fig. 8). The zone between Derinkuyu, Guzelyurt, Mt. Melendiz, and Nigde is surrounded with maxspots with no AS anomalies in it (Fig. 8). Although the high heat flow and high radiogenic heat production zone is located in the E–W (or slightly NW–SE) direction, different than the NE–SW alignment of AS-free zone (limited by the horizontal gradients), the largest contours are in the superposed form with this AS-free zone. It is also consistent with the deeper parts of the 3D model map indicating the shallow structure of Cappadocia (Kosaroglu et al. 2016). To indicate the relationship between the surface topography and subsurface structures, a block diagram is presented in Fig. 10. Mt. Melendiz and Mt. Hasan both have uplift indications in the subsurface and they are surrounded by a depression. The corridor extending in the northeast of Mt. Melendiz's root through the SW of Derinkuyu is a potential geothermal exploration area with its

shallow CPDs and high heat flows together with the high radiogenic heat production zone. This corridor's elongation is in the NW–SE direction until a large subsurface high that was interpreted as the largest plutonic intrusion in the central Anatolia named as the "Baranadag Pluton" in the former paper of authors. In case of determining fault zones and drilling new geothermal wells, Cappadocia could be a new geothermal energy production area in Turkey, in addition to its natural, historical, agricultural, and touristic prosperities.

REFERENCES

Artemieva, I. M., & Money, W. D. (2001). Thermal thickness and evolution of Precambrian lithosphere. *Journal of Geophysical Research, 106,* 16387–16414.

Ates, A., Bilim, F., & Buyuksarac, A. (2005). Curie point depth investigation of Central Anatolia, Turkey. *Pure and Applied Geophysics, 162,* 357–371.

Aydar, E., & Gourgaud, A. (1998). The geology of Mount Hasan stratovolcano, central Anatolia, Turkey. *Journal of Volcanology and Geothermal Research, 85,* 129–152.

Aydemir, A. (2008). Hydrocarbon potential of the Tuzgolu (Salt Lake) Basin, Central Anatolia, Turkey: a comparison of geophysical investigation results with the geochemical data. *Journal of Petroleum Science and Engineering, 61,* 33–47.

Aydemir, A. (2009). Tectonic investigation of central Anatolia., Turkey, using geophysical data. *Journal of Applied Geophysics, 68,* 321–334.

Aydemir, A., & Ates, A. (2005). Preliminary evaluation of Central Anatolian basins in Turkey using the gravity and magnetic data. *Journal of the Balkan Geophysical Society, 8,* 7–19.

Aydemir, A., & Ates, A. (2006). Structural interpretation of the Tuzgolu and Haymana Basins, Central Anatolia, Turkey, using seismic, gravity and aeromagnetic data. *Earth, Planets and Space, 58,* 951–961.

Ayhan, A.K., & Papak, I. (1988). *Aksaray-Taspinar-Altınhisar-Ciftlik-Delihebil (Nigde) civarinin jeolojisi.* MTA Report No. 8315 (unpublished).

Baldwin, R. T., & Langel, R. (1993). Tables and maps of the DGRF 1985 and IGRF 1990, international union of geodesy and geophysics association of geomagnetism and aeronomy. *IAGA Bulletin, 54,* 158.

Bas, H., Guner, Y., & Emre, O. (1986). Erciyes Dagi volkanit-lerinin ozellikleri. Selcuk Universitesi. *Mühendislik Mimarlık Fakültesi Dergisi, 1,* 29–44.

Batum, I. (1978a). Nevsehir GB Golludag ve Acigol yoresi volkanitlerinin jeolojisi ve petrografisi. *Hacettepe Yerbilimleri Dergisi, 3,* 50–69.

Batum, I. (1978b). Golludag ve Acigol volkanitlerinin jeokimyasi ve petrolojisi. *Hacettepe Yerbilimleri Dergisi, 3,* 70–88.

Besang, C., Eckhardt, F. J., Harre, W., Kreuzer, H., & Muller, P. (1977). Radiometrische Altersbestimmungen an Neogenen Eruptivgsteinen der Turkei. *Geologisches Jahrbuch, 25,* 3–36.

Bigazzi, G., Yegingil, Z., Ercan, T., Oddone, M., & Ozdogan, M. (1993). Fission track dating obsidians of Central and Northern Anatolia. *Bulletin of Volcanology, 55,* 588–595.

Bilim, F., & Ates, A. (2003). Analytic Signal inferred from reduced to the pole data. *Journal of the Balkan Geophysical Society, 6,* 66–74.

Bilim, F., & Ates, A. (2005). Analitik Sinyal yontemlerinin man-yetik model verileri uzerinde karsilastirilmasi. *Istanbul niversitesi Mühendislik Fakültesi Yerbilimleri Dergisi, 18,* 151–162. **(in Turkish with English Abstract)**.

Bilim, F., Akay, T., Aydemir, A., & Kosaroglu, S. (2016). Curie point depth, heat flow and radiogenic heat production deduced from the spectral analysis of the aeromagnetic data for geother-mal investigation on the Menderes Massif and the Aegean Region, western Turkey. *Geothermics, 60,* 44–57.

Bingol, E. (1974). 1:2500 000 olcekli Turkiye metamorfizma har-itasi ve bazi metamorfik kusaklarin jeoteknik evrimi uzerine tartismalar. *MTA Bulletin, 83,* 178–184.

Blakely, R. J. (1996). *Potential theory in gravity and magnetic applications.* Cambridge: Cambridge University Press.

Buyuksarac, A., Jordanova, D., Ates, A., & Karloukovski, V. (2005). Interpretation of the Gravity and Magnetic anomalies of the Cappadocia Region, Central Turkey. *Pure and Applied Geophysics, 162,* 2197–2213.

Dolmaz, M. N., Hisarli, Z. M., Ustaomer, T., & Orbay, N. (2005a). Curie point depths based on spectrum analysis of the aeromag-netic data, West Anatolian Extensional Province, Turkey. *Pure and Applied Geophysics, 162,* 571–590.

Dolmaz, M. N., Ustaomer, T., Hisarli, Z. M., & Orbay, N. (2005b). Curie Point Depth variations to infer thermal structure of the crust at the African-Eurasian convergence zone, SW Turkey. *Earth Planets Space, 57,* 373–383.

Ekingen, A. (1982). *Nevsehir kalderasinda jeofizik prospeksiyon sonuclari* (p. 82). Turkiye Jeoloji Kurultayi: Abstract Book.

Froger, J. L., Lenat, J. F., Chrowicz, J., Le Pennec, J. L., Bourdier, J. L., Kose, O., et al. (1998). Hidden calderas evidenced by multisource geophysical data; example of Cappadocian Calderas, Central Anatolia. *Journal of Volcanology and Geothermal Research, 185,* 99–128.

Frost, B. R., & Shive, P. N. (1986). Magnetic mineralogy of the lower continental crust. *Journal of Geophysical Research, 91,* 6513–6521.

Hsieh, H. H., Chen, C. H., Lin, P. Y., & Yen, H. Y. (2014). Curie point depth from spectral analysis of magnetic data in Taiwan. *Journal of Asian Earth Sciences, 90,* 26–33.

Hunt, C.P., Moskowitz, B.M., & Banerjee, S.K. (1995). Magnetic properties of rocks and minerals. In: T.J. Ahrens (Ed.), *Rock physics and phase relations: a handbook of physical constants* (pp. 189–204). American Geophysical Union.

Ilkisik, M., Gurer, A., Tokgoz, T., & Kaya, C. (1997). Geoelec-tromagnetic and geothermic investigations in the Ihlara Valley Geothermal Field. *Journal of volcanology and geothermal Research, 78,* 297–308.

Innocenti, F., Mazzuoli, G., Pasquare, F., Radicati Di Brozolo, F., & Villari, L. (1975). The Neogene calcalkaline volcanism Cen-tral Anatolia: geochronological data on Kayseri-Nigde area. *Geological Magazine, 112,* 349–360.

Jaupart, C. (1986). On the average amount and vertical distribution of radioactivity in the continental crust. In J. Burrus (Ed.), *Thermal modeling in sedimentary basins* (pp. 33–47). Paris: Editions Technip.

Kosaroglu, S., Buyuksarac, A., & Aydemir, A. (2016). Modeling of shallow structures in the Cappadocia region using gravity and aeromagnetic anomalies. *Journal of Asian Earth Sciences, 124,* 214–226.

Lachenbruch, A. H. (1970). Crustal temperature and heat produc-tion: implication of the linear heat flow relationship. *Journal of Geophysical Research, 75,* 3291–3300.

Le Pennec, J. L., Bourdier, J. L., Froger, J. L., Temel, A., Camus, G., & Gourgaud, A. (1994). Neogene ignimbrites of the Nevsehir plateau (Central Turkey): stratigraphy distribution and source constraints. *Journal of Volcanology and Geothermal Research, 63,* 59–67.

MacLeod, I. N., Jones, K., & Dai, T. F. (1993). 3-D analytic signal in the interpretaiton of total magnetic field data at low magnetic latitudes. *Exploration Geophysics, 24,* 679–688.

Nabighian, M. N. (1972). The analytic signal of two-dimensional magnetic bodies with polygonal cross-section: its properties and use for automated anomaly interpretation. *Geophysics, 37,* 507–517.

Okubo, Y., Graf, R. J., Hansen, R. O., Ogawa, K., & Tsu, H. (1985). Cruie Point Depths of the Island of Kyushu and Sur-rounding Areas, Japan. *Geophysics, 50,* 481–494.

Okubo, Y., Tsu, H., & Ogawa, K. (1989). Estimation of Curie point and geothermal structure of island arcs of Japan. *Tectonophysics, 159,* 279–290.

Okubo, Y., Uchida, Y., Taniguchi, M., Miyakoshi, A., & Safanda, J. (2005). Statistical analysis for thermal data in the Japanese Islands. *Physics of the Earth and Planetary Interiors, 152,* 277–291.

Onal, K. M., Buyuksarac, A., Aydemir, A., & Ates, A. (2008). Investigation of the deep structure of the Sivas Basin with geo-physical methods, Innereast Anatolia, Turkey. *Tectonophysics, 460,* 186–197.

Ortiz-Aleman, C., & Urrutia-Fucugauchi, J. (2010). Aeromagnetic anomaly modeling of central zone structure and magnetic sour-ces in the Chicxulub crater. *Physics of the Earth and Planetary Interiors, 179,* 127–138.

Pasquare, G. (1968). Geology of the Cenozoic volcanic area of Central Anatolia. *Atti Accad Naz Lincei, 9,* 53–204.

Pasquare, G., Poli, S., Vezzoli, L., & Zanchi, A. (1988). Conti-nental arc volcanism and tectonic setting in Central Anatolia, Turkey. *Tectonophysics, 146,* 217–230.

Piper, J. D. A., Gursoy, H., & Tatar, O. (2002). Palaeomagnetism and magnetic properties of the Cappadocian ignimbrite succes-sion, central Turkey and Neogene tectonics of the Anatolian collage. *Journal of Volcanology and Geothermal Research, 117,* 237–262.

Piper, J. D. A., Kocbulut, F., Gursoy, H., Tatar, O., Viereck, L., Lepetit, P., et al. (2013). Palaeomagnetism of the Cappadocian Volcanic Succession, Central Turkey: major ignimbrite emplacement during two short (Miocene) episodes and Neogene

tectonics of the Anatolian collage. *Journal of Volcanology and Geothermal Research, 262,* 47–67.

Platzman, E. S., Tapirdamaz, C., & Sanver, M. (1998). Neogene anticlockwise rotation of Central Anatolia (Turkey): preliminary palaeomagnetic and geochronological results. *Tectonophysics, 299,* 175–189.

Ross, H. E., Blakely, R. J., & Zoback, M. D. (2006). Testing the use of aeromagnetic data for the determination of Curie depth in California. *Geophysics, 71,* L51–L59.

Rozimant, K., Buyuksarac, A., & Bektas, O. (2009). Interpretation of magnetic anomalies and estimation of depth of magnetic crust in Slovakia. *Pure and Applied Geophysics, 166,* 471–484.

Saibi, H., Nishijima, J., Ehara, S., & Aboud, E. (2006). Integrated gradient interpretation techniques for 2-D and 3-D gravity data interpretation. *Earth Planets Space, 58,* 815–821.

Salem, A., Ravat, D., Gamey, T. J., & Ushijima, K. (2002). Analytic signal approach and its applicability in environmental magnetic investigations. *Journal of Applied Geophysics, 49,* 231–244.

Sassano, G. (1964). *Acıgol bolgesinde Neojen ve Kuvaterner Volkanizmasi.* MTA Report No. 6841, Ankara.

Schlinger, C. M. (1985). Magnetization of lower crust and interpretation of regional crust anomalies: example from Lofoten and Vesteralen, Norway. *Journal of Geophysical Research, 90,* 11484–11504.

Seymen, I. (1982). *Kaman dolayinda Kirsehir Masifi'nin jeolojisi.* TPAO Report No. 1836 (unpublished).

Spector, A., & Grant, F. S. (1970). Statistical models for interpretation aeromagnetic data. *Geophysics, 35,* 293–302.

Springer, M. (1999). Interpretation of heat-flow density in the Central Andes. *Tectonophysics, 306,* 377–395.

Stampolidis, A., & Tsokas, G. N. (2002). Curie point depths of Macedonia and Thrace, N. Greece. *Pure and Applied Geophysics, 159,* 2659–2671.

Tanaka, A., Okubo, Y., & Matsubayashi, O. (1999). Curie point depth based on spectrum analysis of the magnetic anomaly data in east and southeast Asia. *Tectonophysics, 306,* 461–470.

Temel, A., Gundogdu, M. N., Gourgaud, A., & Le Pennec, J. L. (1998). Ignimbrites of Cappadocia (Central Anatolia, Turkey): petrology and Geochemistry. *Journal of Volcanology and Geothermal Research, 85,* 447–471.

Tezcan, A. K., & Turgay, M. I. (1987). *Heat flow density distribution in turkey.* Ankara: Publ. MTA.

Toprak, V. (1998). Vent distribution and its relation to regional tectonics, Cappadocian volcanics, Turkey. *Journal of Volcanology and Geothermal Research, 85,* 55–67.

Tsokas, G. N., Hansen, R. O., & Fytikas, M. (1998). Curie point depth of the island of Crete (Greece). *Pure and Applied Geophysics, 152,* 747–757.

Turcotte, D. L., & Schubert, G. (1982). *Geodynamics: Applications of continuum physics to geological problems.* New York: Wiley.